

Evidence for $\bar{\nu}_\mu \rightarrow \bar{\nu}_e$ Oscillations from the LSND Experiment at the Los Alamos Meson Physics Facility

C. Athanassopoulos,¹² L. B. Auerbach,¹² R. L. Burman,⁷ I. Cohen,⁶ D. O. Caldwell,³ B. D. Dieterle,¹⁰ J. B. Donahue,⁷
A. M. Eisner,⁴ A. Fazely,¹¹ F. J. Federspiel,⁷ G. T. Garvey,⁷ M. Gray,³ R. M. Gunasingha,⁸ R. Imlay,⁸ K. Johnston,⁹
H. J. Kim,⁸ W. C. Louis,⁷ R. Majkic,¹² J. Margulies,¹² K. McIlhany,¹ W. Metcalf,⁸ G. B. Mills,⁷ R. A. Reeder,¹⁰
V. Sandberg,⁷ D. Smith,⁵ I. Stancu,¹ W. Strossman,¹ R. Tayloe,⁷ G. J. VanDalen,¹ W. Vernon,^{2,4} N. Wadia,⁸ J. Waltz,⁵
Y-X. Wang,⁴ D. H. White,⁷ D. Works,¹² Y. Xiao,¹² S. Yellin³

LSND Collaboration

¹University of California, Riverside, California 92521

²University of California, San Diego, California 92093

³University of California, Santa Barbara, California 93106

⁴University of California Intercampus Institute for Research at Particle Accelerators, Stanford, California 94309

⁵Embry Riddle Aeronautical University, Prescott, Arizona 86301

⁶Linfield College, McMinnville, Oregon 97128

⁷Los Alamos National Laboratory, Los Alamos, New Mexico 87545

⁸Louisiana State University, Baton Rouge, Louisiana 70803

⁹Louisiana Tech University, Ruston, Louisiana 71272

¹⁰University of New Mexico, Albuquerque, New Mexico 87131

¹¹Southern University, Baton Rouge, Louisiana 70813

¹²Temple University, Philadelphia, Pennsylvania 19122

(Received 9 May 1996)

A search for $\bar{\nu}_\mu \rightarrow \bar{\nu}_e$ oscillations has been conducted at the Los Alamos Meson Physics Facility by using $\bar{\nu}_\mu$ from μ^+ decay at rest. The $\bar{\nu}_e$ are detected via the reaction $\bar{\nu}_e p \rightarrow e^+ n$, correlated with a γ from $np \rightarrow d\gamma$ (2.2 MeV). The use of tight cuts to identify e^+ events with correlated γ rays yields 22 events with e^+ energy between 36 and 60 MeV and only 4.6 ± 0.6 background events. A fit to the e^+ events between 20 and 60 MeV yields a total excess of $51.0^{+20.2}_{-19.5} \pm 8.0$ events. If attributed to $\bar{\nu}_\mu \rightarrow \bar{\nu}_e$ oscillations, this corresponds to an oscillation probability of $(0.31 \pm 0.12 \pm 0.05)\%$. [S0031-9007(96)01375-0]

PACS numbers: 14.60.Pq, 13.15.+g

We present the results from a search for neutrino oscillations using the Liquid Scintillator Neutrino Detector (LSND) apparatus described in Ref. [1]. The existence of neutrino oscillations would imply that neutrinos have mass and that there is mixing among the different flavors of neutrinos. Candidate events in a search for the transformation $\bar{\nu}_\mu \rightarrow \bar{\nu}_e$ from neutrino oscillations with the LSND detector have previously been reported [2] for data taken in 1993 and 1994. Data taken in 1995 have been included in this paper, and the analysis has been made more efficient.

Protons are accelerated by the Los Alamos Meson Physics Facility (LAMPF) linac to 800 MeV kinetic energy and pass through a series of targets, culminating with the A6 beam stop. The primary neutrino flux comes from π^+ produced in a 30-cm-long water target in the A6 beam stop [1]. The total charge delivered to the beam stop while the detector recorded data was 1787 C in 1993, 5904 C in 1994, and 7081 C in 1995. Neutrino fluxes used in our calculations include upstream targets and changes in target configuration during these three years of data taking.

Most of the π^+ come to rest and decay through the sequence $\pi^+ \rightarrow \mu^+ \nu_\mu$, followed by $\mu^+ \rightarrow e^+ \nu_e \bar{\nu}_\mu$, supplying $\bar{\nu}_\mu$ with a maximum energy of 52.8 MeV. The energy dependence of the $\bar{\nu}_\mu$ flux from decay at rest

(DAR) is very well known, and the absolute value is known to 7% [1,3]. The open space around the target is short compared to the pion decay length, so only 3% of the π^+ decay in flight (DIF). A much smaller fraction (approximately 0.001%) of the muons DIF, due to the difference in lifetimes and that a π^+ must first DIF. The total $\bar{\nu}_\mu$ flux averaged over the detector volume, including contributions from upstream targets and all elements of the beam stop, was $7.6 \times 10^{-10} \bar{\nu}_\mu/\text{cm}^2/\text{proton/}$.

A $\bar{\nu}_e$ component in the beam comes from the symmetrical decay chain starting with a π^- . This background is suppressed by three factors in this experiment. First, π^+ production is about 8 times the π^- production in the beam stop. Second, 95% of π^- come to rest and are absorbed before decay in the beam stop. Third, 88% of μ^- from π^- DIF are captured from atomic orbit, a process which does not give a $\bar{\nu}_e$. Thus the relative yield, compared to the positive channel, is estimated to be $\sim (1/8) \times 0.05 \times 0.12 = 7.5 \times 10^{-4}$. A detailed Monte Carlo simulation [3] gives a value of 7.8×10^{-4} for the flux ratio of $\bar{\nu}_e$ to $\bar{\nu}_\mu$.

The detector is a tank filled with 167 metric tons of dilute liquid scintillator, located about 30 m from the neutrino source and surrounded on all sides except the bottom

by a liquid scintillator veto shield. The dilute mixture allows the detection in photomultiplier tubes (PMTs) of both Čerenkov light and isotropic scintillation light, so that reconstruction provides robust particle identification (PID) for e^\pm along with the e^\pm position and the direction of the event. PID is based on the quality of the position and Čerenkov angle fits and on the relative amount of early light [1]. The detector needs to distinguish between events induced by $\bar{\nu}_e$ (oscillation candidates) from the events produced by the ν_e . LSND detects $\bar{\nu}_e$ via $\bar{\nu}_e p \rightarrow e^+ n$, a process with a well-known cross section [4], followed by the neutron-capture reaction $np \rightarrow d \gamma$ (2.2 MeV). Thus the oscillation event signature consists of an “electron” signal, followed by a 2.2 MeV photon correlated with the electron signal in both position and time. Detection of DAR ν_e in LSND is dominated by charged current reactions on ^{12}C , but an electron from $\nu_e \ ^{12}\text{C} \rightarrow e^- \ ^{12}\text{N}$ has energy $E_e < 36$ MeV because of the mass difference of ^{12}C and the lowest lying ^{12}N state. Moreover, the DAR production of a correlated photon from $\nu_e \ ^{12}\text{C} \rightarrow e^- \ n \ ^{11}\text{N}$ can occur only for $E_e < 20$ MeV because of the threshold for free neutron production.

Cosmic rays are suppressed at the trigger level by use of the veto shield and by rejecting events with any evidence for a muon in the previous $15.2 \mu\text{s}$ [1]. Even so, the trigger rate is dominated by this background, with actual ν -induced events contributing less than $\sim 10^{-5}$ of all triggers. Because the data acquisition and triggering [1] do not depend on whether the beam is on or off, the beam-on to beam-off duty ratio could be measured from triggered events; it averaged 0.070 ± 0.001 over the three years of data. The beam-unrelated background in any beam-on sample is thus well measured from the much larger beam-off sample and can be subtracted. The cuts used to select e^+ candidates are designed to discriminate heavily against this background, so that the statistical error from this subtraction can be kept small relative to the beam-dependent signal.

Separation of correlated neutron-capture photons from accidental signals is achieved using an approximate likelihood ratio R [2,5] for the correlated and accidental hypotheses. R is defined using distributions [5] of the number of hit PMTs for the reconstructed γ and of the time and distance between the primary event and that γ .

These three “correlated γ ” distributions are found to be approximately independent of the primary event location in the fiducial volume. Nevertheless, the R distribution is determined from the position distribution of the events when fitting the data. For purposes of fitting, the R distribution for accidental photons is taken from γ s in the last $250 \mu\text{s}$ of the 1 ms γ window and from laser calibration events. That for correlated photons is taken from cosmic ray neutron events either directly or as modified for the lower-energy neutrons of interest by using a Monte Carlo simulation of the distance distribution, with fit results averaged over the two cases.

We present analysis of the full 1993 + 1994 + 1995 data sample for two sets of positron selection cuts. Selection I (see Table I) corresponds to the criteria used in our previous paper on the 1993 and 1994 data [2]. The 1995 data increase integrated delivered beam by a factor of 1.9, with a corresponding increase in backgrounds to 4.3 ± 0.5 events using selection I cuts; the total number of corresponding candidate events is increased from 9 to 13. Selection VI uses new insight into the nature of the beam-off backgrounds to further reduce these backgrounds while relaxing other criteria to increase the signal efficiency by about 40%. The criteria were chosen, and efficiencies determined, using several control samples taken as part of the data stream. A sample of “Michel” electrons from the decays of stopping cosmic ray muons is used to characterize energy calibration, resolution, and PID. Cosmic ray neutrons stopping in the detector are used for the 2.2 MeV γ properties and as a “nonelectron” control sample for electron PID. Other neutrino induced interactions in the detector including $\nu_\mu \ ^{12}\text{C} \rightarrow \mu^- X$ [6] and $\nu_e \ ^{12}\text{C} \rightarrow e^- X$ are also used to check efficiencies and backgrounds. Random triggers in association with tank calibration are used to determine veto efficiencies, readout dead time, and the distribution of R for accidentally coincident γ .

The primary particle in a $\bar{\nu}_e$ event candidate is required to have a PID consistent with a positron. The selection I criteria for PID were previously described [2], giving an efficiency for positrons in the $36 < E_e < 60$ MeV energy range of 0.77 ± 0.02 . Selection VI loosens the PID criteria to increase PID efficiency to 0.84 ± 0.02 .

Selection I removed all events with the time to the previous triggered event $\Delta t_p < 50 \mu\text{s}$ to eliminate Michel

TABLE I. The number of signal and background events in the $36 < E_e < 60$ MeV energy range. E/F is the excess number of events divided by the total efficiency. The beam-off background has been scaled to the beam-on time. VIb is a restrictive geometry test.

Selection	Signal	Beam-Off	ν Bkgd.	Excess	E/F
I $R \geq 0$	221	133.6 ± 3.1	53.5 ± 6.8	33.9 ± 16.6	130 ± 64
I $R > 30$	13	2.8 ± 0.4	1.5 ± 0.3	8.7 ± 3.6	146 ± 61
VI $R \geq 0$	300	160.5 ± 3.4	76.2 ± 9.7	63.3 ± 20.1	171 ± 54
VI $R > 30$	22	2.5 ± 0.4	2.1 ± 0.4	17.4 ± 4.7	205 ± 54
VIb $R \geq 0$	99	33.5 ± 1.5	34.3 ± 4.4	31.2 ± 11.0	187 ± 66
VIb $R > 30$	6	0.8 ± 0.2	0.9 ± 0.2	4.3 ± 2.5	110 ± 63

electrons from muon decay. Selection VI required Δt_p greater than $20 \mu\text{s}$, and no activities between 20 and $34 \mu\text{s}$ before the event trigger time with more than 50 PMT hits or reconstructed within 2 m from the positron position. The selection I and VI efficiencies are 0.50 ± 0.02 and 0.68 ± 0.02 , respectively. The time to any subsequent triggered event, Δt_a , is required to be $> 8 \mu\text{s}$ to remove events which are misidentified muons which decay (0.99 ± 0.01 efficiency). The reconstructed positron location was required to be a distance $D > 35$ cm from the surface tangent to the faces of the PMTs (0.85 ± 0.05 efficiency). This assures that the positron is in a region of the tank in which the energy and PID responses vary smoothly and are well understood. The 35 cm cut also avoids the region of the tank with the highest cosmic ray background.

To suppress cosmic ray neutrons, the number of associated γ with $R > 1.5$ is required to be no more than two for selection I (0.99 ± 0.01 efficiency) and no more than one for selection VI (0.94 ± 0.01 efficiency). Recoil neutrons from the $\bar{\nu}_e p \rightarrow e^+ n$ reaction are too low in energy to knock out additional neutrons. The number of veto shield hits associated with the events is no more than one for selection I (0.84 ± 0.02 efficiency) and no more than three for selection VI (0.98 ± 0.01 efficiency).

Beam-off data surviving these cuts were found to include cosmic ray events entering the detector tank from outside. We have found two new criteria which are effective at reducing this background. One is the distribution of angles between the e^+ direction and its position vector relative to the tank center—background events tend to head inwards. The other is in the distribution of veto hits—cosmic ray events tend to have more of them. These two distributions are used in a way analogous to the R parameter discussed earlier in defining a likelihood ratio, S [5]. For selection VI, but not I, we require $S > 0.5$, a cut that loses 13% of the expected neutrino signal while eliminating 33% of the beam-off background. Including a 0.97 ± 0.01 data acquisition efficiency gives overall efficiencies of 0.26 ± 0.02 for selection I and 0.37 ± 0.03 for selection VI.

The backgrounds to $\bar{\nu}_e p \rightarrow e^+ n$ followed by n capture fall into three general classes: beam-off events (cosmic ray induced), beam-related events with correlated neutrons, and beam-related events with an accidental γ . As outlined above, the cosmic ray background to beam-on events is 0.07 times the number of beam-off events which pass the same criteria. The major sources of beam-induced backgrounds are from μ^- DAR, discussed above, and from π^- DIF in the beam stop. The latter results in a background from $\bar{\nu}_\mu p$ interactions where the final μ^+ is missed, and its Michel decay positron is mistaken for a primary $\bar{\nu}_e p$ event. These $\bar{\nu}_\mu$ backgrounds are estimated using the detector Monte Carlo simulation [1,5]. The backgrounds with accidental γ overlap are greatly reduced by selection on the R parameter. Details of all backgrounds considered are presented in Ref. [5].

Table I lists the number of signal, beam-off-background, and neutrino-background events for the two selections with $36 < E_e < 60$ MeV—to avoid large accidental- γ backgrounds. The likelihood ratio R is used to determine whether a candidate 2.2 MeV γ is correlated with an electron or from an accidental coincidence. Requiring $R > 30$ (correlated- γ efficiency = 0.23) we observe 22 events beam-on and $36 \times 0.07 = 2.5$ events beam-off. The estimated beam-related background consists of 1.72 ± 0.41 events with correlated neutrons and 0.41 ± 0.06 without. The probability that the beam-on events are entirely due to a statistical fluctuation of the 4.6 ± 0.6 event expected total background is 4.1×10^{-8} . Figure 1(a) shows the energy distribution of all primary electrons which pass selection VI with associated $R \geq 0$. Figure 1(b) shows the electron energy distribution for selection VI with $R > 30$.

Kolmogorov tests have been done to check for unexpected concentrations of events in position (e.g., in regions of high cosmic ray or γ backgrounds), energy, or time (year). No consistency check yields a probability so low as to demonstrate a serious inconsistency [5]. A restrictive geometric cut, removing the 55% of the selection VI acceptance with highest cosmic ray rates [5,7], also demonstrates no inconsistency; its results are labeled VIb in Table I.

To determine the oscillation probability we fit the overall R distribution, for events satisfying selection VI, in the full energy range $20 < E_e < 60$ MeV. The larger energy range is used in this and the following fit to utilize the maximum amount of data and is made possible by our increased understanding of the background processes. The 1763 beam-on and 11981 beam-off events were fit by a χ^2 method which took spatial variations in accidental photon rates into account by averaging the appropriate R distributions at the positions of each positron. The result of

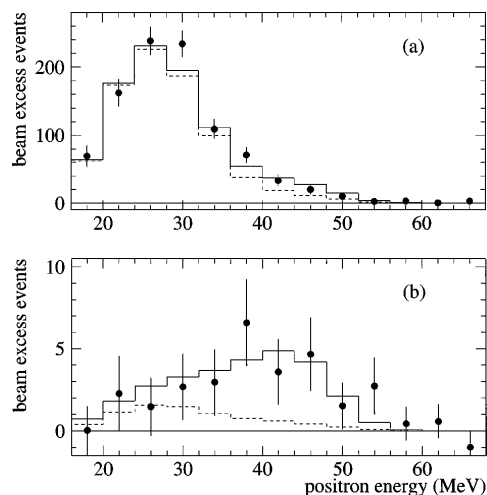


FIG. 1. The energy distribution for events which pass selection VI with (a) $R \geq 0$ and (b) $R > 30$. Shown in the figure are the beam-excess data, estimated neutrino background (dashed), and expected distribution for neutrino oscillations at large Δm^2 plus estimated neutrino background (solid).

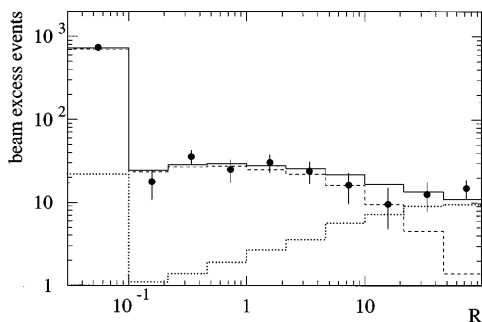


FIG. 2. The R distribution, beam-on minus beam-off excess, for events that satisfy selection VI and that have energies in the range $20 < E_e < 60$ MeV. The solid curve is the best fit to the data, the dashed curve is the uncorrelated γ component of the fit, and the dotted curve is the correlated γ component.

the fit is shown in Fig. 2. It yielded $63.5^{+20.0}_{-19.3}$ beam-related events with a correlated γ and $861.6^{+20.0}_{-19.5}$ beam-related events without a correlated γ . The latter is consistent with a calculated background estimate of 795 ± 134 such events. Subtracting the estimated neutrino background with a correlated γ (12.5 ± 2.9 events) results in a net excess of $51.0^{+20.2}_{-19.5}$ events, corresponding to an oscillation probability of $(0.31 \pm 0.12 \pm 0.05)\%$, where the second error is systematic. A likelihood fit which uses individual local accidental- γ R distributions for each positron gave a consistent result of $(0.30 \pm 0.12 \pm 0.05)\%$.

For simplicity we present the results in the two-generation formalism, in which the mixing probability is written as $P = \sin^2 2\theta \sin^2(1.27\Delta m^2 L/E_\nu)$, where θ is the mixing angle, Δm^2 is the difference of the squares of the two mass eigenstates in eV^2 , L is the distance from neutrino production in meters, and E_ν is the neutrino energy in MeV. An overall likelihood fit has been made to determine favored regions in the Δm^2 vs $\sin^2 2\theta$ parameter space for two-neutrino mixing. The fit was made to distributions in the observed event energy, the neutron likelihood ratio R , the reconstructed direction of the electron relative to the neutrino beam direction, and the distance of the primary event from the beam stop neutrino source. The beam-related and cosmic ray backgrounds were added to the expected neutrino oscillation signal, and a likelihood was calculated for a range of Δm^2 vs $\sin^2 2\theta$ values. Figure 3 shows regions which are within 2.3 and 4.5 log-likelihood units of the maximum. These values are motivated by the fact that they would define 90% and 99% confidence level regions, respectively, for a two-dimensional Gaussian likelihood function. They do not define exact confidence limits but show the regions favored by the experiment. The favored regions have been enlarged to account for systematic effects by varying the inputs to the fit to reflect uncertainty in backgrounds, neutrino fluxes, and the R distribution shape. Figure 3 also shows the 90% C.L. limits from KARMEN [8] (dashed curve), E776 (dotted curve) [9], and the Bugey reactor [10] (dot-dashed curve).

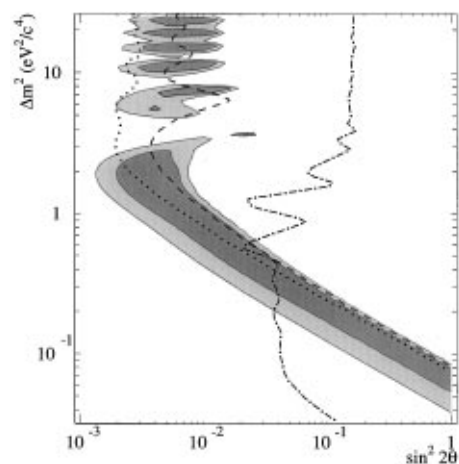


FIG. 3. Plot of the LSND Δm^2 vs $\sin^2 2\theta$ favored regions. The shaded regions are the favored likelihood regions as defined in the text. Also shown are 90% C.L. limits from KARMEN at ISIS (dashed curve), E776 at BNL (dotted curve), and the Bugey reactor experiment (dot-dashed curve)

This paper reports the observation of 22 electron events in the $36 < E_e < 60$ MeV energy range that are correlated in time and space with a low-energy γ with $R > 30$, and the total estimated background from conventional processes is 4.6 ± 0.6 events. The probability that this excess is due to a statistical fluctuation is 4.1×10^{-8} . A fit to the full energy range $20 < E_e < 60$ MeV gives an oscillation probability of $(0.31 \pm 0.12 \pm 0.05)\%$. These results may be interpreted as evidence for $\bar{\nu}_\mu \rightarrow \bar{\nu}_e$ oscillations within the favored range of Fig. 3.

This work is conducted under the auspices of the US Department of Energy, supported in part by funds provided by the University of California for the conduct of discretionary research by Los Alamos National Laboratory. This work is also supported by the National Science Foundation.

- [1] C. Athanassopoulos *et al.*, Nucl. Instrum. Methods (to be published).
- [2] C. Athanassopoulos *et al.*, Phys. Rev. Lett. **75**, 2650 (1995).
- [3] R. L. Burman, M. E. Potter, and E. S. Smith, Nucl. Instrum. Methods Phys. Res., Sect. A **291**, 621 (1990); R. L. Burman, A. C. Dodd, and P. Plischke, Nucl. Instrum. Methods Phys. Res., Sect. A **368**, 416 (1996).
- [4] C. H. Llewellyn Smith, Phys. Rep. **3**, 262 (1972); P. Vogel, Phys. Rev. D **29**, 1918 (1984); E. J. Beise and R. D. McKeown, Comm. Nucl. Part. Phys. **20**, 105 (1991).
- [5] C. Athanassopoulos *et al.*, Phys. Rev. C (to be published).
- [6] M. Albert *et al.*, Phys. Rev. C **51**, 1065 (1995).
- [7] J. Hill, Phys. Rev. Lett. **75**, 2654 (1995).
- [8] B. Bodmann *et al.*, Phys. Lett. B **267**, 321 (1991); B. Bodmann *et al.*, Phys. Lett. B **280**, 198 (1992); B. Zeitnitz *et al.*, Prog. Part. Nucl. Phys. **32**, 351 (1994).
- [9] L. Borodovsky *et al.*, Phys. Rev. Lett. **68**, 274 (1992).
- [10] B. Achkar *et al.*, Nucl. Phys. **B434**, 503 (1995).